Multifractal structure of medium energy particles in p-AgBr interactions at 800 GeV

R. K. Shivpuri, Geetanjali Das, and Simi Dheer
Department of Physics and Astrophysics, University of Delhi, Delhi 110 007, India

S. K. Soni
Department of Physics, Shri Guru Tegh Bahadur Khalsa College, University of Delhi, Delhi 110 007, India
(Received 27 June 1994)

We present the experimental results on multifractal structure of medium energy particles in 800-GeV proton-AgBr interactions. We observe a power-law dependence of the multiplicity moments on mean multiplicity in varying bin widths of the angular distribution. The experimental values of generalized dimensions are determined from the slopes for two different categories of interactions in different multiplicity regions. The observed behavior of generalized dimensions D_q and of the related singularity spectrum shows a consistent departure from randomness and is a typical multifractal. The observations support a possible cascading mechanism in the emission process of target fragmented medium energy protons. The inhomogeneity of the probability distribution measured by the difference $1 - D_q$ decreases with increase in the average multiparticle density.

PACS number(s): 13.85.Hd, 24.60.Ky, 29.40.Rg

I. INTRODUCTION

The notion of anomalously large rapidity fluctuations of nonstatistical origin in the small bin size regime called intermittency has its genesis in turbulent flow. The concept of intermittency is in turn intimately related to multifractal geometry [1] of the underlying production processes. Multifractality has been the focal point of a number of theoretical investigations [2,3] on dynamics of multiparticle production. The question arises if one should study intermittency and multifractality in nuclear fragmentation processes using the same tool, i.e., dependence of suitable moments on the bin size of the distribution variable. A first step in this direction has been taken by Ploszajczak and Tucholski [4], who have investigated intermittent behavior in nuclear fragmentation at intermediate energies by studying the bin size dependence of normalized factorial moments of the fragment-size distributions in bins of varying electric charges.

Until now, all the investigations on multifractality have been carried out only for the production processes of the high-energy hadrons (pionization region). It would be interesting to explore if the medium-energy particles produced in nuclear fragmentations also follow a multifractal structure. This will not only provide a unified description of the whole production process but also provide an additional parameter to understand the dynamics of particle production phenomena.

We use for our analysis the target fragmented medium-energy protons, observed in proton interactions with AgBr nuclei in emulsion at 800 GeV, which is presently the highest energy for fixed targets.

Takagi [5] has proposed a simple new multifractal measure to probe the multifractal structure of multiparticle production in proton-antiproton and electron-positron interactions and studied its linear behavior as a function of logarithm of the resolution. Takagi has argued that the departure from predicted linear behavior in a log-log plot of bin size and the well-known G_q moments [2,3] may be because the number of points (particles) in most experiments do not strictly approach infinity. This requirement is overcome in Takagi's approach [5], where the number of points can be made arbitrarily large by taking a large number of events. Using the measure proposed by Takagi [5], our data for medium-energy particles show a linear behavior over a broad range of resolutions. Generalized dimensions D_q characteristic of such a behavior have been determined from slopes. The difference $1 - D_q$ is a measure of nonstatistical fluctuations present in the interaction processes. The statistical fluctuations are suppressed because of the large bin size. The variation of D_q with q is clearly in favor of multifractal geometry suggestive of a possible cascading phenomena in the emission processes of target fragmented medium-energy protons. The behavior of generalized dimensions gives a measure of the inhomogeneity in the probability distribution. We have also studied the spectrum of singularities of the probability distribution, i.e., how the probability of picking up a singularity scales with resolution.

II. EXPERIMENTAL DETAILS

A stack of 40 Ilford G5 emulsion pellicles of dimension $10 \times 8 \times 0.06$ cm^3 was exposed to a proton beam of energy 800 GeV at Fermilab. The beam flux was 8.7×10^4 particles/cm^2. The scanning of interactions was done under a 40× objective of the high-resolution microscopes by the area scanning method. Using the double-scan data, the scanning efficiency was calculated for each observer and the overall efficiency was found to be greater than

90%. In order to make sure that the interactions are due to beam only, all the interactions were followed back. The interactions lying within 25 μm each from the air and the glass surface have not been considered for measurement purposes. Following the above criteria, 3500 events were scanned.

All the charged secondaries of these events were classified according to the nuclear emulsion terminology [6]. Secondary tracks having $I \leq 1.4I_0$, $\beta(v/c) \geq 0.7$ were designated as shower tracks, those having $10\ I_0 \geq I > 1.4I_0$, $0.7 > \beta \geq 0.3$ were designated as grey tracks and black tracks have $I > 10I_0$, $\beta < 0.3$, where I and I_0 are the ionizations of secondary and primary tracks, respectively. The values of N_s, N_g, and N_b denote the multiplicities of shower, grey, and black tracks, respectively. The shower tracks are due to fast particles produced in the elementary nucleon-nucleon collisions. The heavy tracks (N_h) include the grey and black tracks. The former are mostly due to medium-energy (30–400 MeV) knockon nucleons, whereas the latter are produced by low-energy target fragments resulting from evaporation of the nucleus.

The measurement of the angles of the secondary tracks with respect to the beam axis was done by the coordinate method under a 100× oil immersion objective. The values of x, y, and z coordinates at the vertex and two points each on the grey and beam tracks were measured. The emission angle (Θ) for each grey track was calculated using the three-dimensional (3D) coordinate geometry method. The uncertainty in angle measurement was determined to be $\sim 10^{-4}$ rad. It has been shown [7,8] that N_g is a better parameter than N_h to reflect the type of target in emulsion. The parameter $\bar{\nu}(N_g)$ [8,9] measures the average number of collisions of the primary during its traversal within the nucleus. The value of $\bar{\nu}(N_g)$ has been parametrized [9] by

$$\bar{\nu}(N_g) = 2.2\sqrt{N_g}\ . \tag{1}$$

Hence, by confining our study to $N_g > 3$ events, the minimum value of $\bar{\nu}(N_g)$ is = 4.4. The value of $\bar{\nu}(N_g)$ for the CNO and AgBr groups of nuclei has been shown [10] to be = 2.1 and 3.2, respectively. Thus the events considered by us are all in the heavy nucleus category, viz., the AgBr targets. Further, this is also clear from the value of N_h which has been used [6] to reflect the number of nucleons that have participated in the interaction. Events with $N_h \geq 9$ are unambiguously due to AgBr targets. The events considered in the present analysis have predominantly $N_h \geq 9$. In the following we shall omit the subscript g in N_g for convenience and from now on, we shall discuss the grey track distribution only. The total number of events with at least one grey track was found to be 1544. Out of the entire event sample, events with $N \leq 3$ were not considered since in such events it becomes difficult to disentangle the statistical noise from dynamical fluctuations. To study the role of the multiplicity in multifractality we categorize the entire event sample with the above cut into two regions, namely $N \leq 6$ and $N > 6$, which have average multiplicities 4.93 and 8.77, respectively.

III. DATA ANALYSIS, RESULTS, AND DISCUSSION

Figure 1 shows a plot of average shower multiplicity against the number of medium-energy protons. Due to low statistics events with $N > 10$ have not been plotted. It is evident from Fig. 1 that there is a strong correlation of these protons with the produced shower particles. Hence one would surmise that these target-associated particles would also carry information of the underlying production process. The multiparticle density distribution of fast produced particles in a single event shows a characteristic chaotic behavior over a broad range of resolutions. It would be interesting to explore if the medium-energy protons also exhibit such a chaotic behavior. The usual longitudinal distribution variable pseudorapidity is not suitable for the study of these particles as they are heavier than pions and also less energetic. Following other workers [11] we choose cosine of emission angle ($\cos\Theta$) as the basic distribution variable in our analysis. The parameter $\cos\Theta$ will hereinafter be referred to as w.

Following considerations analogous to those recently presented by Takagi [5] to explain multiparticle production, let us consider an emission process of medium-energy protons at a given incident energy and their distribution in w space.

A. Method

In order to analyze bin-size dependence of the fluctuations present in the angular distribution of grey tracks, we consider a single-variable bin of length l in w space. As a measure of density fluctuations we consider a multifractality function

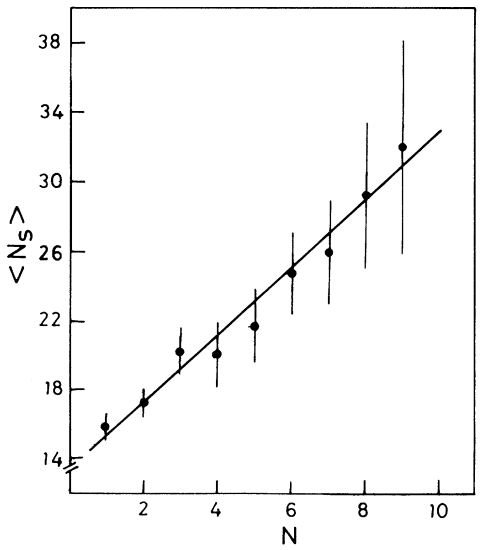

FIG. 1. Average shower multiplicity, $\langle N_s \rangle$, as a function of grey multiplicity N. The least-squares fit is shown by the solid line.

$$H_g(l) = \frac{1}{q-1}\ln\left(\frac{\langle N(l)^q\rangle}{\langle N(l)\rangle}\right) , \quad (2)$$

where $q > 0$. $N(l)$ is the bin multiplicity of grey tracks, and angular brackets stand for event average. The case $q = 1$ is obtained by taking the appropriate limit in Eq. (2):

$$H_1(l) = \lim_{q\to 1} H_q(l) = \frac{\langle N(l)\ln N(l)\rangle}{\langle N(l)\rangle} . \quad (3)$$

To diagnose multifractal geometry of the underlying process we vary the bin width of angular distribution and study the behavior of the quantities $H_q(l)$ as a linear function of logarithm of $\langle N(l)\rangle$, i.e.,

$$H_q(l) = A_q + D_q \ln\langle N(l)\rangle , \quad (4)$$

where A_q and D_q are constants independent of l. If such a scale-invariant behavior holds for a broad range of "resolutions" [5] $\langle N(l)\rangle$, then this is a diagnostic indicator of fractal geometry and the scaling exponent D_q is identified as a generalized dimension of such a set. The quantity D_0 is the fractal dimension of the set. The information dimension D_1 quantifies the bin-size dependence of the information entropy. For integral values $q = 2, 3, 4 \ldots$, generalized dimensions have a simple physical interpretation [12] as scaling exponents of q-particle correlations.

The slope of the $H_q(l)$ vs $\ln\langle N(l)\rangle$ plot yields a generalized dimension for any $q > 0$. If q is different from unity, Eq. (4) implies a linear relation of the form [5]

$$\ln\langle N(l)^q\rangle = (q-1)A_q + [(q-1)D_q + 1]\ln\langle N(l)\rangle . \quad (5)$$

On the other hand, in the limit of $q = 1$, Eq. (4) reduces to a linear relation of the form [5]

$$\frac{\langle N(l)\ln N(l)\rangle}{\langle N(l)\rangle} = A_1 + D_1 \ln\langle N(l)\rangle , \quad (6)$$

where D_1 is the information dimension. Equations (5) and (6) will be used to determine D_q for any real positive q value. In order to determine the statistical contribution, we proceed as follows [13–16]. We distribute the secondary tracks randomly throughout the interval $L = [-1, +1]$ and then determine $\langle N(l)^q\rangle_{\rm st}$ by averaging

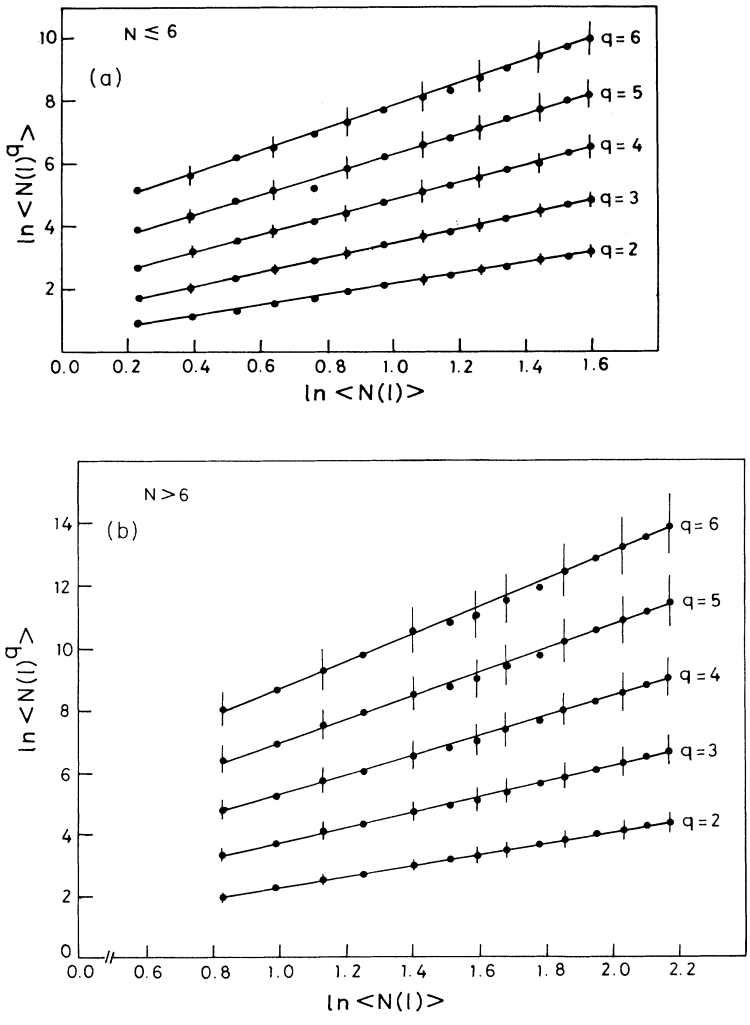

FIG. 2. Bin-size dependence of moments of multiplicity distribution of medium-energy particles in (a) $N \leq 6$ and (b) $N > 6$ interactions. The least-squares fits are indicated by the solid lines.

TABLE I. Values of slopes B_q and intercepts A_q (parenthesis) from least-squares fits of Eq. (9) to the data for the two multiplicity regions. The errors are standard.

Category	B_2 (A_2)	B_3 (A_3)	B_4 (A_4)	B_5 (A_5)	B_6 (A_6)
$N \leq 6$					
Observed values	1.708 ± 0.008	2.293 ± 0.013	2.780 ± 0.017	3.189 ± 0.022	3.534 ± 0.031
	(0.480 ± 0.009)	(0.596 ± 0.007)	(0.697 ± 0.006)	(0.784 ± 0.006)	(0.860 ± 0.007)
Noise effect	2.0 ± 0.0	3.0 ± 0.0	4.0 ± 0.0	5.0 ± 0.0	6.0 ± 0.0
	(2.190 ± 0.001)	(2.230 ± 0.0)	(2.282 ± 0.0)	(2.345 ± 0.0)	(2.412 ± 0.0)
$N > 6$					
Observed values	1.794 ± 0.012	2.496 ± 0.027	3.144 ± 0.044	3.760 ± 0.060	4.356 ± 0.075
	(0.478 ± 0.020)	(0.605 ± 0.023)	(0.708 ± 0.024)	(0.794 ± 0.025)	(0.866 ± 0.025)
Noise effect	2.0 ± 0.0	3.0 ± 0.0	4.0 ± 0.0	5.0 ± 0.0	6.0 ± 0.0
	(1.705 ± 0.0)	(1.771 ± 0.0)	(1.848 ± 0.0)	(1.929 ± 0.0)	(2.010 ± 0.0)

over the observed multiplicity distribution $P(N)$. Following Chiu, Fialkowski, and Hwa [13] we have used the following multinomial distribution for estimating the background:

$$P_N(n_1, n_2, \ldots, n_m) = \frac{N!}{n_1! n_2! \cdots n_m!} \left(\frac{1}{M}\right)^N \delta n_1 + n_2 + \cdots n_m, N, \quad (7)$$

where M is the number of bins into which L is divided. Substituting (7) into the following relation, we have determined the statistical component present in our data:

$$\langle N(l)^q \rangle_{\rm st} = \sum_N P(N) \sum_{n_1,\ldots,n_m} N(l)^q P_N(n_1, \ldots, n_m) \, . \quad (8)$$

For such randomly distributed tracks in events, the generalized dimensions ($q > 0, q \neq 1$) are determined from the slopes of $\ln\langle N(l)^q \rangle_{\rm st}$ vs $\ln\langle N(l) \rangle_{\rm st}$ [see Eq. (5)].

B. Evidence of fractal geometry

We considered a symmetric bin $-l/2 < w < l/2$ in the w variable. Our aim was to compute $\langle N(l) \ln N(l) \rangle / \langle N(l) \rangle$ and $\ln\langle N(l)^q \rangle$ over a broad range of resolutions $\langle N(l) \rangle$ for the data as well as for the corresponding randomized events. We also studied whether the above parameters behave linearly with the logarithm of resolution. To perform our analysis in the large phase-space region, the bin width was varied in steps of 0.1 from 0.7 to 2.0.

We investigated multifractality in the grey track data by considering plots of $\ln\langle N(l)^q \rangle$ $(= 2, 3, 4, 5, 6)$ vs $\ln\langle N(l) \rangle$ in w bins of varying sizes. They are shown in Figs. 2(a) and 2(b) for the two different multiplicity regions. All five moments $\langle N(l)^q \rangle$ vary smoothly with $\langle N(l) \rangle$, according to the parametrization

$$\ln\langle N(l)^q \rangle = (q-1) A_q + B_q \ln\langle N(l) \rangle, \quad (9)$$

where the corresponding values of A_q and B_q are shown in Table I. When this analysis was repeated for ran-

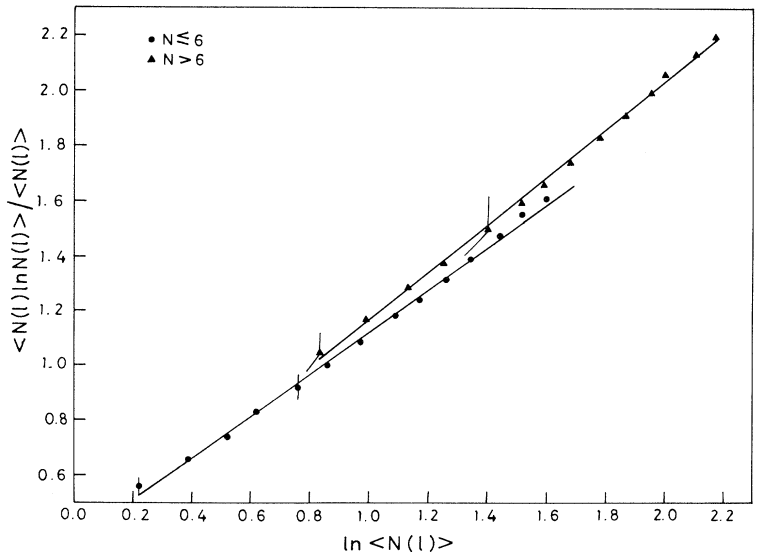

FIG. 3. Plots of $\langle N(l) \ln N(l) \rangle / \langle N(l) \rangle$ vs $\ln\langle N(l) \rangle$ with least-squares fits for $N \leq 6$ and $N > 6$ interactions.

TABLE II. Values of various dimensions (D_q) for the two multiplicity regions. The errors are standard.

Category	D_1	D_2	D_3	D_4	D_5	D_6
$N \leq 6$	0.777 ± 0.012	0.708 ± 0.008	0.646 ± 0.006	0.593 ± 0.006	0.547 ± 0.006	0.507 ± 0.006
$N > 6$	0.856 ± 0.010	0.794 ± 0.012	0.748 ± 0.014	0.715 ± 0.015	0.690 ± 0.015	0.671 ± 0.015

domly distributed tracks in events (assuming a binomial background distribution), the corresponding results for A_q and B_q are also shown in Table I. In the case of statistical background $B_q = q$. The difference $q - B_q$ is a measure of the nonstatistical origin of fluctuations.

The variation in $\langle N(l) \ln N(l)\rangle / \langle N(l)\rangle$ plotted against the logarithm of average grey multiplicity is shown in Fig. 3 where the data points belonging to two multiplicity regions are plotted side by side. These straight lines are represented according to Eq. (6). The values of the intercepts and slopes for $N \leq 6$ are 0.346 ± 0.013, 0.777 ± 0.012 and for $N > 6$ the corresponding values are 0.318 ± 0.016 and 0.856 ± 0.010, respectively.

The foregoing analysis shows the existence of linear relations between $\ln\langle N(l)^q\rangle$ and $\ln\langle N(l)\rangle$, and between $\langle N(l)\ln N(l)\rangle / \langle N(l)\rangle$ and $\ln\langle N(l)\rangle$. This provides evidence for the first time of the presence of a possible fractal geometry in target fragmentation processes resulting in the emission of medium-energy protons in the present interactions.

IV. EXPERIMENTAL VALUES OF FRACTIONAL DIMENSIONS

It is of great interest to characterize the observed fractal pattern by generalized dimensions D_q. The novel feature is that different underlying processes suggest different dependencies of D_q on q. For positive integral q values higher than 1, generalized dimensions D_q are determined from the slopes B_q given in Table I, using [see Eqs. (5) and (9)]

$$D_q = (B_q - 1)/(q - 1) \ . \tag{10}$$

The information dimension D_1 is equal to the value of the slope parameter as given above from Eq. (6). Table II gives the values of generalized dimensions determined by us for the two event samples. The systematics of generalized dimensions will be discussed in the next section. We have extended the above analysis to q values ($0 < q < 0.6$) and tried a linear fit to experimental values of the form

$$D_q = a + bq \ . \tag{11}$$

The values of the intercept (a) and slope (b) parameters for $N \leq 6$ and $N > 6$ are 0.936 ± 0.000, -0.115 ± 0.001, 0.982 ± 0.000, and -0.083 ± 0.001, respectively. Extrapolating to the limit $q = 0$ in Eq. (11) we are led to the remarkable result that D_0 nearly coincides with topological dimension of the set, i.e.,

$$D_0 \simeq 1 \ . \tag{12}$$

This result means that there are practically no empty bins in our analysis.

V. EVIDENCE OF MULTIFRACTALITY AND ITS MULTIPLICITY DEPENDENCE

Our study of the slopes of the multifractality function [see Eq. (2)] computed as a function of the logarithm of mean multiplicity in the w bin of size l has led to a hierarchy of generalized dimensions the top of which is given by the fractal dimension D_0 [see Eq. (12)]. Since the dimensions are not constant, one speaks of anomalous scaling laws of the underlying multifractal geometry. For small q the following relation expected from a lognormal distribution is found to hold:

$$D_q = D_1 - \tfrac{1}{2}\mu(q - 1) \ . \tag{13}$$

The values of μ for the two different categories of interactions are given by 0.274 ± 0.001 and 0.210 ± 0.001 for $N \leq 6$ and $N > 6$, respectively. For q higher than 1, D_q no longer varies linearly with q. Such a behavior clearly supports a cascading mechanism for the underlying pro-

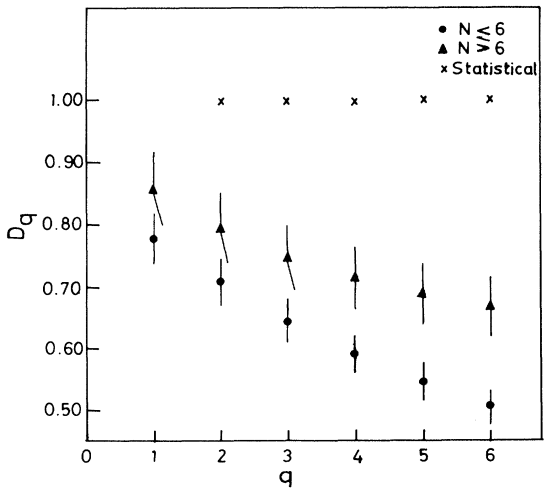

FIG. 4. Distributions of generalized dimensions D_q as a function of q for $N \leq 6$ and $N > 6$ interactions.

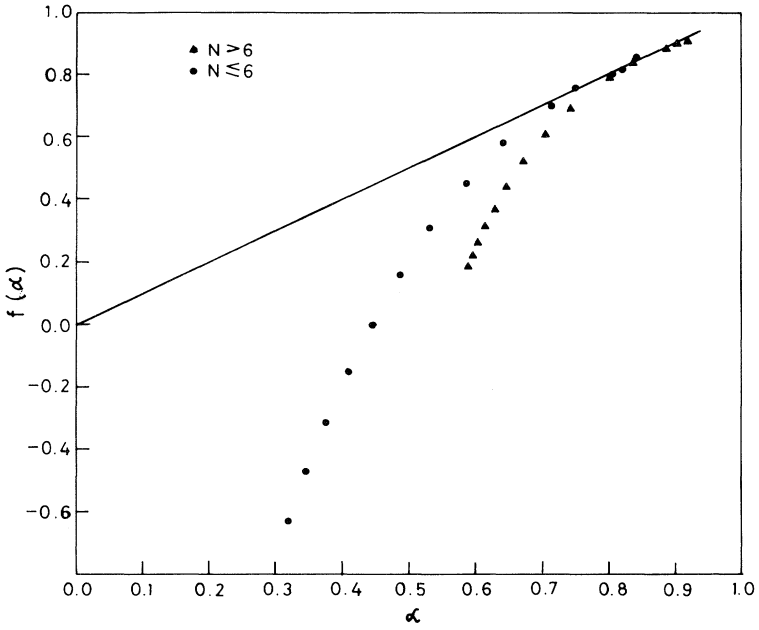

FIG. 5. The singularity spectra $f(\alpha)$ as a function of α for $N \leq 6$ and $N > 6$ interactions. The straight line is the 45° line drawn through the origin.

cess. Intuitively the D_q distribution measures spatial inhomogeneity of the multiparticle density distribution. As the order q varies, the amount of difference $1 - D_q$ provides a measure of this inhomogeneity or multifractality in grey track density distribution. From Table II we see that $1 - D_q$ decreases with increase in the average grey track multiplicity. The behavior of D_q vs q for $q \geq 1$ is shown in Fig. 4. The solid circles and triangles denote the measured values of D_q and the crosses show the results of statistical background. The departure of D_q from 1 shows the presence of nonstatistical fluctuations in the present interactions. For small q values ($q < 1$), D_q vs q shows a linearity and we have not plotted these values.

Following the approach of Halsey *et al.* [17], a multifractal object can be viewed as an interwoven family of different monofractal sets $S(\alpha)$ on which the probability measure has a singularity of the type α. We have studied the spectrum of singularities of the grey track density distribution (measure) by relating the generalized dimensions D_q to the fractal dimensionality $f(\alpha)$ by means of a Legendre transformation

$$f(\alpha) = q\alpha - (q-1)D_q \ . \tag{14}$$

Note that Eq. (14) is equivalent to the relations [see Eq. (10)]

$$\alpha = \frac{dB_q}{dq}, \quad q = \frac{df}{d\alpha} \ . \tag{15}$$

Figure 5 shows the spectrum function $f(\alpha)$ for $N \leq 6$ and $N > 6$ interactions, for $0.6 \leq q \leq 6.0$. For even small-q values we found that the change in the value $f(\alpha)$ is insignificant. The observed $f(\alpha)$ spectrum possesses all the characteristics expected from a multifractal distribution [17]. For small q, the spectrum function is well represented by the curve

$$f(\alpha) = \alpha - \frac{1}{2\mu}(\alpha - D_1)^2 \ , \tag{16}$$

where μ is defined by Eq. (13). Equation (16) is the Legendre transform of Eq. (13). For $q \geq 1$, there is evidence of departure from the typical parabolic shape of Eq. (16). Compared with $N \geq 6$ interactions, the spread of the spectrum function in $N \leq 6$ interactions is more. Hence, the grey track multiplicity behavior is more chaotic in $N \leq 6$ as compared with $N > 6$ interactions.

VI. CONCLUSIONS

In presenting the first experimental results on multifractality in medium-energy protons our main conclusions can be summarized as follows.

In the plots of $\ln\langle N(l)^q\rangle$ vs $\ln\langle N(l)\rangle$ and $\langle N(l)\ln N(l)\rangle/\langle N(l)\rangle$ vs $\ln\langle N(l)\rangle$, linear relations are found to hold, both for $N \leq 6$ and $N > 6$ interactions. This clearly points to the existence of fractality in the target fragmentation process. The contribution of statistical noise to $\langle N(l)^q\rangle$ was determined. This allowed us to disentangle the dynamical from the statistical effects.

The plot of generalized dimension D_q vs q for $q < 1$ shows a linear relation, which when extrapolated to $q = 0$, yields $D_0 \sim 1$. This shows that the empty bins are practically nonexistent. For $q > 1$, D_q does not vary linearly with q. This suggests a cascading mechanism for the underlying process of the particles under study. The parameter $1 - D_q$ decreases with increase in the total average grey track multiplicity.

The broad distributions of the spectrum function, $f(\alpha)$ reflects the multifractal nature of grey track density dis-

tributions. The spread of the distribution is more for $N \leq 6$ as compared to $N > 6$ events. Thus, the grey track multiplicity distribution is more chaotic in $N \leq 6$ in comparison to that for $N > 6$ interactions. Similar conclusions were observed [18] in the case of shower tracks in these interactions. This probably points to the "universality" of the underlying mechanism. This needs more investigation in different interactions at varying primary energies.

ACKNOWLEDGMENTS

We are grateful to Fermi National Accelerator Laboratory, Illinois, for exposure facilities at the Tevatron and Dr. Ray Stefanski for help during exposure of the emulsion stack. We would like to thank Dr. R. Wilkes for processing facilities. Financial assistance from the University Grants Commission, India is gratefully acknowledged.

[1] G. Paladin and A. Vulpiani, Phys. Rep. C **156**, 147 (1987); M. Kohmoto, Phys. Rev. A **37**, 1345 (1988); Tamás Tel, Z. Naturforsch. Teil A 43, 1154 (1988).
[2] R. C. Hwa, Phys. Rev. D **41**, 1546 (1990).
[3] C. B. Chiu and R. C. Hwa, Phys. Rev. D **43**, 100 (1991).
[4] M. Ploszajczak and A. Tucholski, Phys. Rev. Lett. **65**, 1539 (1990).
[5] F. Takagi, Phys. Rev. Lett. **72**, 32 (1994).
[6] C. Gupt, R. K. Shivpuri, N. S. Verma, and A. P. Sharma, Phys. Rev. D **26**, 2202 (1982).
[7] M. K. Hegab and J. Hüfner, Phys. Lett. **105B**, 103 (1981); Nucl. Phys. **A384**, 353 (1982).
[8] E. Stenlund and I. Otterlund, Nucl. Phys. **B198**, 407 (1982).
[9] D. H. Brick *et al.*, Phys. Rev. D **39**, 2484 (1989); **41**, 765 (1990).
[10] A. Abduzhamilov *et al.*, Baton Rouge-Cracow-Moscow-Tashkent Collaboration, Z. Phys. C **40**, 1 (1988).
[11] A. Abduzhamilov *et al.*, Baton Rouge-Cracow-Moscow-Tashkent Collaboration, Phys. Rev. D **39**, 86 (1989).
[12] H. G. E. Hentschel and I. Procaccia, Physica D **8**, 435 (1983).
[13] C. B. Chiu, K. Fialkowski, and R. C. Hwa, Mod. Phys. Lett. A **5**, 2651 (1990).
[14] I. Derado, R. C. Hwa, G. Jansco, and N. Schmitz, Phys. Lett. B **283**, 151 (1992).
[15] K. Sengupta *et al.*, Phys. Rev. D **48**, 3174 (1993).
[16] R. C. Hwa and J. Pan, Phys. Rev. D **45**, 1476 (1992).
[17] T. C. Halsey, M. H. Jensen, L. P. Kadanoff, I. Procaccia, and B. I. Shraiman, Phys. Rev. A **33**, 1141 (1986).
[18] R. K. Shivpuri and V. K. Verma, Phys. Rev. D **47**, 123 (1993).